# ESTIMATION OF SIGNIFICANT WAVE HEIGHT USING THE FEATURES OF CYGNSS DELAY DOPPLER MAP

*Jinwei Bu [1,2], Hyuk Park[2], Kegen Yu [1], and Adriano Camps[2]*

[1]School of Environment Science and Spatial Informatics, China University of Mining and Technology, Xuzhou, China
[2]CommSensLab, Universitat Politècnica de Catalunya (UPC-BarcelonaTech), Barcelona, Spain

IGARSS 2022 - 2022 IEEE International Geoscience and Remote Sensing Symposium | 978-1-6654-2792-0/22/$31.00 ©2022 IEEE | DOI: 10.1109/IGARSS46834.2022.9884806

## ABSTRACT

Significant Wave Height (SWH) is a key parameter to characterize waves, which is typically used in sea state monitoring such as wave forecast to ensure ocean navigation safety. Satellite radar altimeter is probably the primary tool to obtain SWH information. However, it cannot be used for large-scale sea state monitoring unless many of theses satellites are deployed. In this article, we aim to study the potential of Global Navigation Satellite System (GNSS)-Reflectometry (GNSS-R) in SWH measurement based on spaceborne Delay-Doppler Maps (DDMs) data. First, 3 observables (i.e., Delay-Doppler Map Average (DDMA), leading edge slope (LES) of normalized integrated delay waveform (NIDW) (LES-NIDW), and trailing edge slope (TES) of NIDW (TES-NIDW) derived from the DDMs are introduced for SWH estimation. Then, an empirical SWH retrieval model is proposed based on three observables. Subsequently, ERA5 SWH is used as reference data to verify the performance of the proposed model. The experimental results show that the Root Mean Square Error (RMSE) and Correlation Coefficient (CC) estimated by SWH of the three observables are better than 0.54 m and 0.88 m, respectively. Among them, the estimation performance based on DDMA observable is the best, with RMSE and CC of 0.49 m and 0. 89 m. This study shows the potential of spaceborne GNSS-R in SWH retrieval.

***Index Terms***—Global Navigation Satellite System-Reflectometry (GNSS-R), Delay-Doppler Maps, observables, significant wave height (SWH), empirical model.

## 1. INTRODUCTION

Significant wave height (SWH) is an important index to describe sea state. Accurate sea state information plays an important role in wave prediction, navigation safety and ocean dynamics. However, traditional measurement methods, such as buoy or traditional X-band radar remote sensing (RS) technology, have small measurement range and high cost [1]. As a relating RS technology, GNSS reflectometry (GNSS-R) can perform all-weather, global coverage with short revisit time in high resolution. At present, GNSS-R technology has been applied to sea surface wind speed retrieval, sea ice detection, ocean altimetry measurements, soil moisture retrieval, e.g., as studied in [2], [3], [4], [5, 6], flood detection [7], ionospheric scintillation monitoring [8], and rainfall detection [9, 10], either, and so on.

As a key application of GNSS-R technology, SWH estimation has also aroused great research interest. In 2004, Soulat et al. [11] conducted a shore-based experiment and proposed for the first time, a semi-empirical method of using the correlation time function of the Interference Complex Field (ICF) of the GNSS reflected signal and the direct signal to retrieve the SWH of the sea waves. In 2007, Alpers and Hasselmann [12] established a linear relationship between the SWH and the square root of the signal-to-noise ratio (SNR) of the SAR echo signal. Peng and Jin also estimated the global ocean SWH using spaceborne Cyclone Global Navigation Satellite System (CYGNSS) GNSS-R data for the first time based on this relationship model [13], However, the SWH retrieval model based on SNR observable adopted in [13] may not be suitable for Spaceborne GNSS-R SWH estimation because the scattering mechanisms of spaceborne GNSS-R and SAR are different. In 2015, Alonso-Arroyo et al. used GNSS-R Interference Pattern Technique (IPT) to retrieve SWH and Mean Sea Surface Level (MSSL). The shore based experiment results show that the accuracy of SWH and MSSL estimated by this method is 6 cm and 4 cm [14]. Unfortunately, the current research on SWH based on Spaceborne GNSS-R is very limited, existing studies usually carry out spaceborne GNSS-R SWH retrieval based on SNR method. Although the method is simple, the model retrieval performance needs to be further improved. To expand the application of different DDM observables in spaceborne GNSS-R SWH estimation, it is necessary to conduct an in-depth research on other observables in addiont to the SNR observable.

In this study, the potential of GNSS-R in SWH retrieval is studied by using the observables obtained from GNSS-R Delay-Doppler maps (DDMs) observed by CYGNSS satellite. Firstly, the quality of DDM data is strictly controlled in order to improve the accuracy of SWH retrieval. Then, three observables are calculated from CYGNSS DDM data, and an empirical model of SWH is proposed based on these three observables. Finally, the results of the proposed method are compared with ERA5 SWH data.

## 2. DATASET DESCRIPTION AND DATA PROCESSING

### 2.1 Dataset

In this study, two data sets are introduced: the GNSS-R L1 data of CYGNSS satellite, and reanalyzed the SWH data of

European Center for medium range weather forecasts (ECMWF).

At present, the National Aeronautics and Space Administration (NASA) mainly opens three levels (i.e., L1, L2, and L3) of CYGNSS GNSS-R data to users. The L1 data records the DDM, reflection point coordinates, transmitter position and other relevant information of the 8 CYGNSS satellites (i.e., CY01, CY02, CY03, CY04, CY05, CY06, CY07 and CY08), download from (https://podaac-tools.jpl.nasa.gov/drive/files/allData/cygnss/L3/v3.0). At present, this version mainly contains GNSS-R data from August 1, 2018 (DOY is 213) to 2021. Considering the large amount of data, we only downloaded the GNSS-R data observed by 8 satellites from April 15, 2020 to May 15, 2020 for our study.

Moreover, ECMWF SWH product is used as reference data for training models and validating models. The Copernicus Climate Change Service (C3S) Climate Database provides users with free access to the ECMWF reanalysis data product at https://www.ecmwf.int/en/forecasts/datasets/browse-reanalysis-datasets. At present, the latest product is ERA5 data, with a temporal resolution of 1 h, and a spatial resolution of 0.5° × 0.5°.

### 2.2 Quality control

To ensure the quality of the CYGNSS data, the CYGNSS L1 version 3.0 measurements are quality controlled before the training model, according to the following criteria [15].

1) The observables need to have good quality, which is determined by the Quality Control (QC) flag in the data.

2) The observables, as well as the SWH matchups, need to be positive (that is, the observables are greater than 0).

3) The measurements taken when the star tracker is not tracking due to solar contamination are discarded.

4) The measurements from the GPS Block type II-F satellites are discarded, due to the lack of accurate information on the transmitter antenna gain pattern for this family of GPS satellites.

5) Data with specular reflection points more than 25 km far away from the land are selected to reduce the modeling error.

6) Observable data range is defined as 38°N–38°S in the latitude.

### 2.3 GNSS-R Observables Calculation

In this study, the DDMA, the LES-NIDW, and the TES-NIDW observables derived from the DDMs are used for spaceborne GNSS-R SWH retrieval. Their definitions are as follows.

*1) DDMA (Delay-Doppler Map Average):* computed as the mean value of the normalized DDM samples within a box defined from the position of the DDM maximum value $(p,q)$. The box expands from $p-1$ to $p+1$ delay bins and $q-2$ to $q+2$ frequency Doppler bins.

*2) LES-NIDW (leading edge slope of normalized integrated delay waveform):* computed as the absolute value of the slope of the Doppler-integrated waveform from the delay bins $[p-1:p]$.

*3) TES-NIDW (trailing edge slope of normalized integrated delay waveform):* computed as the absolute value of the slope of the Doppler-integrated waveform from the delay bins $[p:p+1]$.

It should be noted that in this study, the delay and Doppler ranges are determined to be [−0.25 0.25] chips, and [−1000 1000] Hz, respectively.

## 3. DEVELOPMENT OF SPACEBORNE GNSS-R SWH MODEL

### 3.1 Modeling Methods

As described in section 2.2, after quality control of DDM data, we can obtain high-quality DDM data. We calculated 3 useful GNSS-R observables from DDM, and the data of ERA5 SWH product is matched to the specular point position of CYGNSS through a bilinear interpolation in space and linear interpolation in time by using the data acquisition time and the specular point location of DDM. The data are further divided into training data set, and test data randomly. The 60 % of the data samples are used as the training set, and the remaining 40 % of the data samples are used as the test set. Next, three GNSS-R observables and SWH are used as input and output variables, respectively, and the SWH model is established by least squares fitting. Then, the GNSS-R observables of the test data are input into the obtained model, so that the SWH estimation based on the GNSS-R method can be obtained. Finally, to further verify the SWH retrieval performance of the proposed model, the SWH retrieval results of GNSS-R data are compared with ERA5 SWH product.

### 3.2 Modeling Using DDMA, LES, and TES Observables

This section presents an empirical SWH retrieval model using the three 3 observables (DDMA, LES-NIDW, and TES-NIDW) derived from DDMs. The mathematical expression of the model is as follows.

$$SWH_{ob} = A \times {x_{ob,i}}^{B} + C \tag{1}$$

where $x_{ob}$ represents the 3 observables, other symbols are the fitting parameters of the model, and the model fitting parameters are shown in Table 1.

Fig. 1 shows the SWH retrieval empirical model trained with ERA5 SWH data and three observables. In the figure, the scattering density points represent the corresponding relationship between GNSS-R observations and ERA5 SWH values, and the red dotted line is the SWH retrieval empirical model fitted by the training data. The figure also shows the root mean square error (RMSE) and determination coefficient ($R^2$) of the fitting model to evaluate the fitting performance of the model. In addition, we can clearly see that the model based on the three observables has good fitting performance

(less than 0.485 m), and the fitting model has high correlation (better than 0.79) with the scattered data.

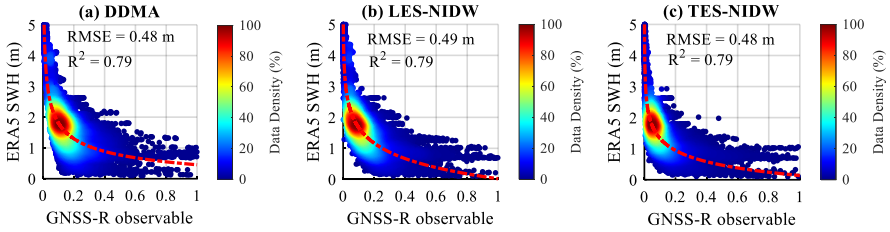


Fig. 1. SWH retrieval models depicted by the dashed magenta line. The colors indicate data density relative to the distribution peak.

**Table 1:** Parameters of SWH Retrieval Models

| Observables | $A$ | $B$ | $C$ |
|---|---|---|---|
| DDMA | 1.39 | -0.2961 | -0.9371 |
| LES-NIDW | 43.63 | -0.01616 | -43.61 |
| TES-NIDW | 5.042 | -0.09244 | -4.906 |

## 4. Model Validation

### 4.1 Assessment performance index

The Root Mean Square Error (RMSE), the Mean Absolute Error (MAE), the Pearson Correlation Coefficient (CC), and the Mean Absolute Percentage Error (MAPE) are used to evaluate the performance of SWH retrieval. The calculation formula of the four indicators is as follows.

$$RMSE = \sqrt{\frac{1}{m}\sum_{i=1}^{m}\left(y_{i,M} - y_{i,T}\right)^2} \tag{2}$$

$$MAE = \frac{1}{m}\sum_{i=1}^{m}\left|y_{i,M} - y_{i,T}\right| \tag{3}$$

$$CC = \frac{\sum_{i=1}^{m}\left(y_{i,M} - \overline{y_M}\right)\left(y_{i,T} - \overline{y_T}\right)}{\sqrt{\sum_{i=1}^{m}\left(y_{i,M} - \overline{y_M}\right)^2 \sum_{i=1}^{m}\left(y_{i,T} - \overline{y_T}\right)^2}} \tag{4}$$

$$MAPE = \frac{1}{m}\sum_{i=1}^{m}\left|\frac{y_{i,M} - y_{i,T}}{y_{i,T}}\right| \times 100\% \tag{5}$$

where $m$ is the number of data samples, $y_{i,M}$ and $y_{i,T}$ are the SWH estimated by the model and the SWH obtained from EAR5 reanalysis data, respectively, $\overline{y_M}$ and $\overline{y_T}$ are the average values of $y_{i,M}$ and $y_{i,T}$, respectively.

### 4.2 Performance Assessment

In this section, SWH is estimated using the empirical model (1) based on the three observables. The retrieval results of the proposed model are verified by ERA5 SWH data. Fig. 2 shows the scatter density plots of ERA5 SWH data and GNSS-R retrieval model estimated SWH. In the figure, the red dotted line is a 1:1 reference line, the green solid line is a linear fitting lines ($Y = aX + b$) between GNSS-R SWH and ERA5 SWH data, the fitting line equation is also shown in the figure. Table 2 also gives four retrieval performance evaluation indexes of the three observables.

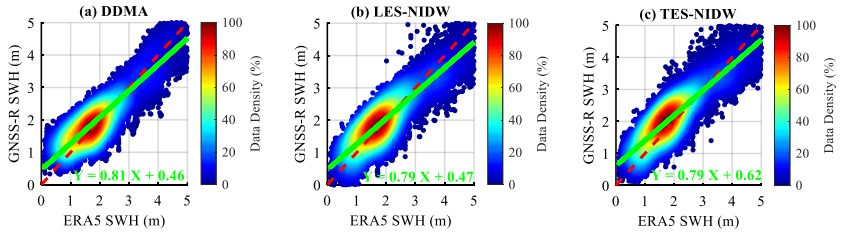


Fig. 2. Retrieval results are validated with ERA5 SWH using the test data set. The red dotted line is the 1:1 reference line, and the green solid line is the linear fitting line of ERA5 SWH data and GNSS-R method model retrieval SWH in the figure. The color bars (from cool to warm) represent the density of the data. (a) DDMA. (b) LES-NIDW. (c) TES-NIDW.

**Table 2:** RMSE, MAE, CC, and MAPE of model-based SWH estimations

| Observables | RMSE (m) | MAE (m) | CC | MAPE (%) |
|---|---|---|---|---|
| DDMA | 0.49 | 0.39 | 0.89 | 30.88 |
| LES-NIDW | 0.51 | 0.39 | 0.88 | 27.62 |
| TES-NIDW | 0.53 | 0.42 | 0.88 | 30.72 |

It can be seen from Fig. 2 and Table 2 that the SWH retrieved by the model developed based on the three observables in this study has good correlation with ERA5 SWH data, and the CC value is better than 0.89. In terms of RMSE and MAE, the retrieval performance of DDMA observable is the best, LES-NIDW observable is the second, and TES-NIDW observable is the worst. In terms of MAPE, LES observable has the best performance, and the other two observables are basically. In general, the retrieval

performance of the SWH model developed based on the three observables is not very different. According to the four evaluation indexes, DDMA observable has obtained better retrieval results, which means that DDMA is more sensitive to sea surface SWH than LES or TES.

To evaluate the retrieval performance of the GNSS-R retrieval model based on three observables under different sea states. Fig. 3 shows the RMSE and MAE of SWH estimates by DDMA, LES-NIDW and TES-NIDW observables under different SWH values. The results of the RMSE and the MAE show that when the SWH is greater than 2 m, the SWH estimation performance of DDMA is better than that of LES-NIDW and TES-NIDW observables. In addition, the figure also shows that the retrieval performance decreases with the increase of SWH value. Therefore, the retrieval performance under high SWH needs to be further improved.

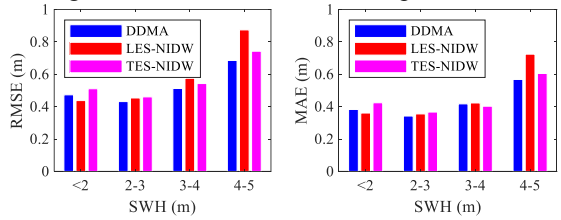


Fig. 3. RMSE and MAE for different ranges of the GNSS-R SWH.

Fig. 4 shows the global distribution of the deviation between GNSS-R SWH and ERA5 SWH data. To facilitate comparison, the deviation has been taken as an absolute value in the figure. We can see that in general, CYGNSS SWH is consistent with ERA5 SWH, showing the feasibility of the proposed method.

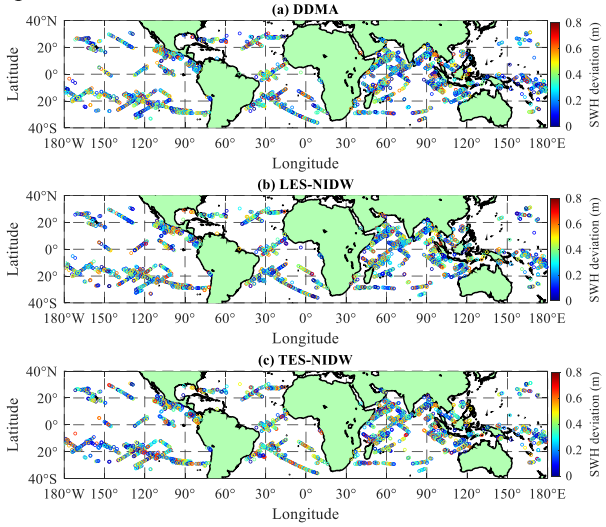


Fig. 4. The distribution of the SWH deviation between the GNSS-R retrieved SWH and ERA5 data. (a) DDMA. (b) LES-NIDW. (c) TES-NIDW.

## 5. CONCLUSIONS

This study conducted the SWH estimation using spaceborne GNSS-R DDM data of CYGNSS mission, devising the SWH retrieval empirical model using three GNSS-R observables (i.e., DDMA, LES, and TES). To verify the performance of the proposed model, the ERA5 SWH data are used to compare and verify the SWH estimation results based on three observables. Among them, the estimation performance based on DDMA observable is the best, with RMSE, MAE, CC and MAPE of 0.49 m, 0.39 m, 0. 89, and 30.9%. The global SWH estimation results also show that the CYGNSS SWH estimation is consistent.

In the future, more data will be exploited to show the feasibility of the SWH estimation. Global coverage of data will be analyzed including various sea states. Additionally, multi-frequency and multi-GNSS reflected signals will be exploited for SWH estimation to further improve the retrieval performance.

## 6. ACKNOWLEDGMENT

This work was supported by the Grant RYC-2016-20918 financed by MCIN/AEI /10.13039 /501100011033 and by ESF Investing in your future.

## 7. REFERENCE

[1] Y. Jia, M. Lin, and Y. Zhang, "Evaluations of the Significant Wave Height Products of HY-2B Satellite Radar Altimeters," *Marine Geodesy,* vol. 43, no. 4, pp. 396-413, 2020.

[2] V. Zavorotny and A. G. Voronovich, "Scattering of GPS Signals from the Ocean with Wind Remote Sensing Application," *IEEE Trans. Geosci. Remote Sens.,* vol. 38, pp. 951-964, 04/01 2000.

[3] D. Llaveria, J. F. Munoz-Martin, C. Herbert, M. Pablos, H. Park, and A. Camps, "Sea Ice Concentration and Sea Ice Extent Mapping with L-Band Microwave Radiometry and GNSS-R Data from the FFSCat Mission Using Neural Networks," *Remote Sens.,* vol. 13, no. 6, 2021.

[4] H. Park, E. Valencia, A. Camps, A. Rius, S. Ribo, and M. Martin-Neira, "Delay Tracking in Spaceborne GNSS-R Ocean Altimetry," *IEEE Geosci. Remote Sens. Lett.,* vol. 10, no. 1, pp. 57-61, 2013.

[5] A. Camps *et al.*, "Sensitivity of GNSS-R Spaceborne Observations to Soil Moisture and Vegetation," *IEEE J. Sel. Top. Appl. Earth Observ. Remote Sens.,* vol. 9, no. 10, pp. 4730-4742, 2016.

[6] A. Camps, H. Park, J. Castellví, J. Corbera, and E. Ascaso, "Single-Pass Soil Moisture Retrievals Using GNSS-R: Lessons Learned," *Remote Sens.,* vol. 12, no. 12, p. 2064, 2020.

[7] S. L. K. Unnithan, B. Biswal, and C. Rüdiger, "Flood Inundation Mapping by Combining GNSS-R Signals with Topographical Information," *Remote Sens.,* vol. 12, no. 18, 2020.

[8] A. Camps, H. Park, G. Foti, and C. Gommenginger, "Ionospheric Effects in GNSS-Reflectometry From Space," *IEEE J. Sel. Top. Appl. Earth Observ. Remote Sens.,* vol. 9, no. 12, pp. 5851-5861, 2016.

[9] M. Asgarimehr, V. Zavorotny, J. Wickert, and S. Reich, "Can GNSS Reflectometry Detect Precipitation Over Oceans?," *Geophys. Res. Lett.,* vol. 45, no. 22, pp. 12585-12592, 2018.

[10] J. Bu and K. Yu, "Sea Surface Rainfall Detection and Intensity Retrieval Based on GNSS-Reflectometry Data from the CYGNSS Mission," *IEEE Trans. Geosci. Remote Sens.,* pp. 1-15, 2021.

[11] F. Soulat, M. Caparrini, O. Germain, P. Lopez-Dekker, M. Taani, and G. Ruffini, "Sea state monitoring using coastal GNSS-R," *Geophys. Res. Lett.,* vol. 31, no. 21, p. L21303, 2004.

[12] W. Alpers and K. Hasselmann, "Spectral signal to clutter and thermal noise properties of ocean wave imaging synthetic aperture radars," *Int. J. Remote Sens.,* vol. 3, no. 4, pp. 423-446, 2007.

[13] Q. Peng and S. Jin, "Significant Wave Height Estimation from Space-Borne Cyclone-GNSS Reflectometry," *Remote Sens.,* vol. 11, no. 5, 2019.

[14] A. Alonso-Arroyo, A. Camps, H. Park, D. Pascual, R. Onrubia, and F. Martin, "Retrieval of Significant Wave Height and Mean Sea Surface Level Using the GNSS-R Interference Pattern Technique: Results From a Three-Month Field Campaign," *IEEE Trans. Geosci. Remote Sens.,* vol. 53, no. 6, pp. 3198-3209, 2015.

[15] M. P. Clarizia and C. S. Ruf, "Statistical Derivation of Wind Speeds From CYGNSS Data," *IEEE Trans. Geosci. Remote Sens.,* vol. 58, no. 6, pp. 3955-3964, 2020.